

Article

Expansive Soil Stabilization Using Alkali-Activated Fly Ash

Huan Wang ^{1,*}, Tengjiao Liu ¹, Chao Yan ¹ and Jianqi Wang ²¹ School of Civil Architecture, Henan University, Kaifeng 475004, China² Xinpu Construction Group Co., Ltd., Zhengzhou 450046, China

* Correspondence: wanghuan@henu.edu.cn

Abstract: Expansive soil swells with water and shrinks with water loss, causing serious safety problems for construction projects. This study emphasizes alkali-activated binder (NaOH excited fly ash) stabilized expansive soil. We found that swelling decreased with an increase in the amount of NaOH in alkali-activated binder. It was found that the alkali-activated binder stabilized expansive soils (AABS) had higher shear strength than untreated expansive soils (US), manifested by increased cohesion and friction angle. In AABS, the highest cohesion and the highest shear strength were found when the NaOH mass was 6% of the fly ash mass. The strength of AABS was similar to that of US without curing. AABS had higher strength than US after 7 and 14 days of curing. The unconfined compressive strength increased with extension of curing time. Combined with XRD and SEM analysis, it was shown that the mechanism of AABS was the formation of C–S–H and (C,N)–A–S–H and the change in the internal structure of expansive soil. This investigation can solve both the expansive soil problem and provide new concepts for green development.

Keywords: expansive soil; alkali-activated binder; unconfined compressive strength; SEM



Citation: Wang, H.; Liu, T.; Yan, C.; Wang, J. Expansive Soil Stabilization Using Alkali-Activated Fly Ash. *Processes* **2023**, *11*, 1550. <https://doi.org/10.3390/pr11051550>

Academic Editors: Juu-En Chang, Yi-Kuo Chang and Jianbo Zhang

Received: 13 April 2023

Revised: 8 May 2023

Accepted: 9 May 2023

Published: 18 May 2023



Copyright: © 2023 by the authors. Licensee MDPI, Basel, Switzerland. This article is an open access article distributed under the terms and conditions of the Creative Commons Attribution (CC BY) license (<https://creativecommons.org/licenses/by/4.0/>).

1. Introduction

Expansive soil is a kind of clay soil that changes with a change in water content. It expands when it meets water and shrinks when it loses water. It has the characteristics of multiple cracks and overconsolidation. A large number of cracks will destroy the integrity of the soil and affect the physical and mechanical properties of the soil. Overconsolidation causes expansive soil to have greater strength and stress [1]. Expansive soils have hydrophilic minerals such as montmorillonite and illite, especially montmorillonite, which exhibits a greater potential for expansion at higher water content and has a higher sensitivity to water [2,3]. The uneven distribution of water in expansive soil leads to a great difference in the expansion and contraction rate of expansive soil, which leads to an irregular distribution of cracks and the instability of the soil after repeated water losses [4]. In the case of a high water content, the soil expands and bulges, making the superstructure rise; when the water content is small, the expansive soil will rapidly depress causing the building to settle, often leading to disasters that cause a serious threat to people and property [5–7]. A common treatment method in construction is to handle expansive soils with lime and cement, which can effectively inhibit the expansion of the soil and provide significant strength increases [5,8]. Unfortunately, these two materials consume large amounts of limestone, electricity and heat in their production, with 7500 J/ton of electricity consumed to make cement [9]. The use of lime and cement produces carbon dioxide, sulfur dioxide and other dust that affects air quality and that have a deleterious impact on the environment. Of these emissions, carbon dioxide accounts for 8–10% of global emissions [10–12]. The search for a new type of modified material with good improvement effects and one that is environmentally green, is therefore particularly important. Alkali-activated binders, also known as alkaline cements, can effectively replace cement and lime to stabilize soils, reducing greenhouse gas emissions by up to 80% compared to Portland cement applications [13]. The alkali excitation process means that the material containing

amorphous silica (SiO_2) and alumina (Al_2O_3) is placed in an alkaline environment, and in a system with high calcium (i.e., more calcium ions are present in the material), the C–A–S–H generated is similar to the C–S–H generated by the hydration of Portland cement [12,14]. C–A–S–H has adhesive properties, which can fill the internal pores of soil and improve the overall strength and durability of soil samples [15]. In this sense, alkali excited industrial waste can replace cement to stabilize expansive soil and other characteristic soils. Recently, alkali-excited industrial wastes have received much attention.

Yi et al. [16] stabilized soft soils using alkali-excited ground granulated blast furnace slag, with Polish special cements as a control group and alkali activator selected as NaOH, CS, Na_2CO_3 , and Na_2SO_4 , respectively. The unconfined compressive strength test (UCS) showed that Na_2CO_3 –GGBS had no stability effect on the soil sample. The strength of NaOH–GGBS was higher than that of cement stabilized clay in the first 90 days, but weaker than that of cement stabilized clay in the later period. The UCS of CS–GGBS stabilized clay at 90 and 180 days was significantly higher than that of cement stabilized clay. The 7-day and 28-day UCS were significantly lower than those of cement-stabilized clay. Rivera et al. [17] found in the SEM test that a dense contact layer was formed between the generated calcium silicate gel and the soil particles, which was caused by the hardening of gel generated by the reaction of volcanic ash. Miraki et al. [18] found that C–S–H and C–A–S–H could be generated under sufficient Ca, Na, Si and Al elements by NaOH excitation of volcanic ash (VA) and slag (GGBS), and the condensation hardening of both could reinforce the internal structure. In the dry and wet cycle test, it was found that with the combination of VA and GGBS, GGBS played a major role, and the soil did not meet the specification requirements when no GGBS was involved. Syed et al. [19] stabilized expansive soils by combined excitation of low-calcium fly ash with NaOH and Na_2SiO_3 showed that alkali-activated binders could improve California bearing ratio (CBR) and UCS by generating filled pores like C–S–H, and reducing swelling by gel wrapping around the surface of soil particles. Adeyanju et al. [20] stabilized soft soils by NaOH excited cement kiln dust (CKD) and CKD + rice husk ash (RHA) revealed that CKD was stronger than CKD + RHA in stabilizing soils. Bruschi et al. [21,22] stabilized the silt by NaOH excitation of sugarcane bagasse ash (SCBA) and carbide lime (CL) which was found to improve strength and durability. The main components of fly ash are SiO_2 and Al_2O_3 , with amorphous and crystalline minerals co-existing in fly ash [23]. It is simply a non-plastic, finely pulverized sand whose composition depends on the type of coal being burned. The current production of fly ash in China greatly exceeds its consumption. In previous studies, it was found that SiO_2 and Al_2O_3 in low calcium fly ash met the requirement of alkali excitation. The new material generated from the activation of fly ash by NaOH is similar to, but not identical to, the product of cement setting and hardening [24,25], so it is believed that the improvement of expansive soil also has the same effect. Alkali-activated binders have a similar effect to cement but are less expensive to produce and more eco-friendly [26,27]. The ability of the generated gel to improve shear and compressive strengths makes AAB promising for application. In China, the utilization rate of low-calcium fly ash is lower due to its own low calcium oxide content. In order to improve the utilization of low-calcium fly ash, this was selected as the material for this test. Hence, this study was conducted to stabilize expansive soil by NaOH excited low calcium fly ash as alkali-activated binders.

2. Materials and Methods

2.1. Materials

The expansive soil in this test was obtained from the northern part of Xinxiang City, Henan Province, and was excavated underground at a distance of 1.5–2 m from the ground surface. The expansive soil at this site contained white and green calcareous nodules inside. The expansive soil was dried for 48 h and then ground, and soil with particle size less than 2 mm was used to prepare for the test, and the geotechnical testing was carried out on the recovered soil samples according to the Standard for Geotechnical Test Methods (GB/T50123-2019), and the basic physical properties of the soil are shown in Table 1.

Table 1. Basic parameters of expansive soils.

Free Swelling Rate	Liquid Limit/%	Plastic Limit/%	Plasticity Index	Maximum Dry Density/(g/cm ³)	Optimum Moisture Content/%	Specific Gravity	Classification of Soil
55	44.52	17.39	27.13	1.61	20	2.76	CH

Fly ash is a pulverized solid formed after burning coal in thermal power plants, which is a waste, and if left untreated will have a negative impact on the environment, and recycling, and its disposal will waste a lot of energy and money. According to Fly ash Used for Cement and Concrete (GB/T1596-2017), the stabilizing agent selected low-calcium fly ash, which was purchased in Xinxiang City. The technical index, loss on ignition values and strength activity index of the selected low-calcium fly ash is Grade 1, 2.4% and 89%, respectively. The chemical composition of fly ash is shown in Table 2. In this study, NaOH (analytical pure) were utilized as alkaline activator solutions. In order to keep the same units in NaOH and fly ash, we chose to add it in solid form.

Table 2. The chemical characterization of fly ash.

Composition	Wight/%
SiO ₂	56.01
Al ₂ O ₃	30.27
Fe ₂ O ₃	4.36
CaO	2.36
K ₂ O	1.71

2.2. Sample Preparation

In this study alkali-excited fly ash as alkali-activated binder (AAB) stabilized expansive soil, the testing was divided into three groups in order to be able to better compare and highlight the advantages of AAB. The first group was untreated expansive soil, named US, and the second group was stable expansive soil with fly ash only, without adding NaOH, named FS. The third group was AAB stabilized expansive soil, after addition of the same fly ash as the second group to the expansive soil, and different masses of NaOH. The mass of NaOH in the third group was 4%, 6%, 8% and 10% of the mass of fly ash. The AAB stabilized soils were named AABS1, AABS2, AABS3 and AABS4 according to the increasing NaOH content. Specific material percentages are shown in Table 3.

Table 3. Percentage of materials in different groups.

Notation	Expansive Soil, wt. %	Fly Ash, wt. %	NaOH, wt. %	W/s
Untreated expansive soil (US)	100	0	0	0.2
Fly ash stabilized expansive soil (FS)	91	9	0	0.2
AAB stabilized expansive soil (AABS1)	90.64	9	0.36	0.2
AAB stabilized expansive soil (AABS2)	90.46	9	0.54	0.2
AAB stabilized expansive soil (AABS3)	90.28	9	0.72	0.2
AAB stabilized expansive soil (AABS4)	90.1	9	0.9	0.2

In this study, soil samples were prepared with reference to the standard for Geotechnical Test Methods (GB/T50123-2019). The expansive soil and fly ash used in the tests were dried in an oven at 110 degrees C. After cooling, the expansive soil was ground with a rubber hammer and stone mortar and passed through a 2 mm sieve, and the soil with a

particle size of less than 2 mm was prepared for sample making. The expansive soil and fly ash were mixed in accordance with the proportions required in Table 3 and dissolved with the weighed NaOH in water. After waiting for the exothermic reaction to finish, the solution was mixed with the solid and stirred well. It was then sealed for one day to finish the samples. Different specimens were prepared according to different tests. The swelling test and the straight shear test required the mixed soil to be made into specimens with a diameter of 61.8 mm and a height of 20 mm. The unconfined compressive strength test required the specimens to be made with a diameter of 39.1 mm and a height of 80 mm. After demolding, it was placed in a curing oven at a temperature of 20 ± 2 °C with an humidity of more than 95% and cured according to the test plan.

2.3. Experimental Work

In this experiment, the effect of AAB on the swelling of expansive soils was measured using two swelling tests, and the effect on the shear strength and compressive strength of expansive soils was measured by two mechanical tests. The unloaded swelling rate test was performed by placing the soil sample in water, limiting the lateral deformation and allowing only upward swelling, and expressing the swelling by the height of upward growth. The loaded swelling rate was measured using the upward height swelling under the influence of the upper load after the soil sample was placed in water, limiting the lateral deformation and placing a fixed load on the upper part of the soil sample. The straight shear test was performed by shearing the soil sample at four different vertical pressures to obtain the shear strength and derive the cohesion and friction angle from the molar circle. The unconfined compressive strength is a method that quickly measures the compressive strength of soil. This test compares the growth of compressive strength under different curing times by unconfined compressive strength. XRD offers useful information on structure, phase, texture and other structural parameters [28,29]. XRD analysis was performed using a Burker LYNXEYE diffractometer to determine the mineralogy of untreated expansive soils and AAB treated soils. The scanning speed was $0.08^\circ/\text{s}$ and the scanning angle was $5^\circ\text{--}70^\circ$. The microstructural changes of the specimens were analyzed by scanning electron microscopy (SEM) and the effect of adding AAB to the expansive soil was analyzed. Scanning electron microscopy analysis of soil surface morphology used field emission scanning electron microscopy. The surface of the soil samples were magnified 500 times, 1000 times, 2000 times and 3000 times, respectively [30].

3. Results and Discussion

3.1. Unloaded Swelling Rate Test

In order to reduce the test error, the swelling tests were taken for each group of three specimens in parallel, and the average value was taken as the final result. Figure 1 shows the results of the unloaded swelling rate test for each group. The unloaded swelling rate of US is 9.1% and the unloaded swelling rate of FS is 7.3%. The addition of fly ash to expansive soils can reduce the unloaded swelling rate by 1.8%. It was believed that fly ash had a smaller particle diameter and larger specific surface area, which could fill the pores of clay better and inhibit the entry of water. In all AABS, the unloaded swelling rate becomes smaller compared to FS. The unloaded swelling rates of AABS1, AABS2, AABS3, and AABS4 were 5.97%, 5.23%, 4.75%, and 4.51%. Compared to FS, the unloaded swelling rate decreased by 3.13%, 3.87%, 4.35% and 4.59%. The difference in the unloaded swelling rate between FS and AABS1 is 1.33%, while the difference in the unloaded swelling rate between AABS3 and AABS4 is only 0.24%. It is believed that the NaOH content in AABS had an effect on the swellability of the clay, and a smaller NaOH content can promote the reduction of swelling. It was found that alkali excitation could cause the unloaded swelling rate to decrease, but the rate of decrease appeared to slow down as the NaOH content increased. this is in accordance with reference [31]. Therefore, there should exist an optimal value of alkalinity in AAB to achieve the optimal economy and effect.

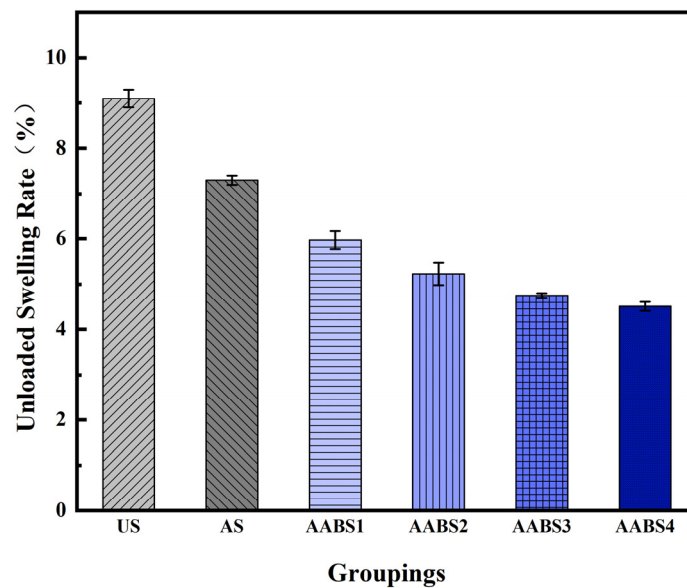


Figure 1. The results of the unloaded swelling rate tests for each group.

3.2. Load Swelling Rate Test

When the load exists in the upper part of the expansive soil, the gravity of the load can produce a certain inhibitory effect on the expansiveness of the expansive soil. The overlying loads were set at 25 kPa and 50 kPa for this experiment. The test results are shown in Figure 2 below. The swelling rate was 2.63 kPa for US and 1.82 kPa for FS when the overlying load was 25 kPa, and the swelling rate decreased by 0.81 kPa when there was no alkali excitation. When the overlying load of all samples was 25 kPa, the swelling rates of AABS1, AABS2, AABS3, and AABS4 were 1.12%, 0.56%, 0.36%, and 0.18%, respectively, which were 0.7%, 1.26%, 1.46%, and 1.64% lower compared to the swelling rate of FS. Although NaOH can make the swelling rate decrease further, it still has certain swelling properties under a 25 kPa overburden load. The swelling rate is 1.46 kPa for US and 1.06 kPa for FS when the overlying load is 50 kPa, and the swelling rate decreases by 0.4 kPa. The expansibility of AABS2 and AABS3 is almost 0, indicating that there is no expansibility at this point, and the expansion force is consistent with the upper pressure. When the overlying load was 50 kPa, the swelling rate of AABS4 was -0.07% . It is indicated that AABS4 can be considered as non-swelling when the upper load is greater than 50 kPa. Because the force generated by the swelling is less than the gravity of the upper load, the swelling is suppressed and cannot be generated. Comprehensive analysis of the two swelling tests shows that both FS and AABS can reduce the swelling of expansive soils, and AAB has a better effect.

The analysis shows that on the one hand, FS reduces the expansibility because fly ash does not have the expansibility itself, but replaces part of the expansive material and covers the clay with a large specific surface area, which prevents part of the water from entering the soil interior and thus restrains the expansion of the soil sample. On the other hand, fly ash contains more high valence ions, Ca^{2+} and Mg^{2+} replace Na^{+} and K^{+} inside the expansive soil, which makes the double electron layer thinner, thus reducing the generation of swelling stress. Because low calcium fly ash has less calcium oxide content and poor early activity, it cannot react with silica and alumina in the soil interior, so fly ash mainly relies on pore filling and ion exchange to reduce swelling [19,32].

The analysis concluded that in AABS, NaOH can provide a strong alkaline environment, which induces the chemical reaction of amorphous silica and alumina in fly ash to generate substances such as N-A-S-H, C-S-H, which enhance the connection between soil interiors and between soil and fly ash, and these hydration products gradually solidify and

harden under maintenance, and fill the soil interiors, creating a water-induced swelling effect. The inhibition of water-induced swelling is achieved [33].

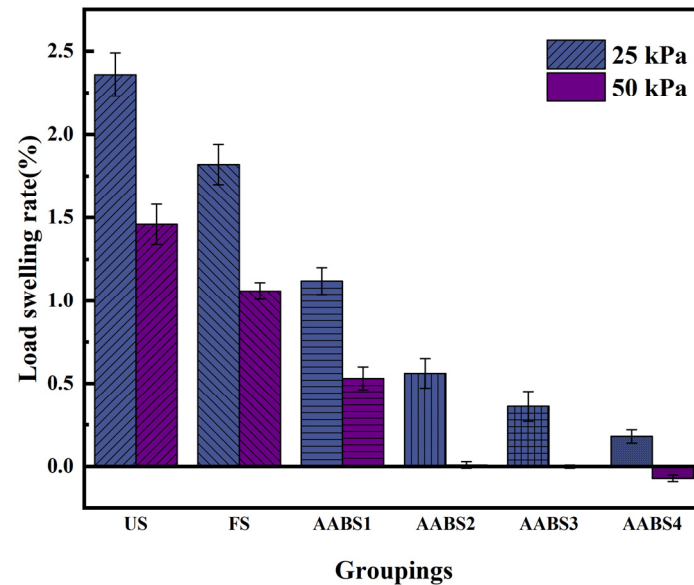


Figure 2. The results of the loaded swelling rate test for each group.

3.3. Direct Shear Test

Figure 3 shows the shear strength values of each group of soil samples under different vertical pressures after 7 days of curing. The shear strength of US was the lowest, the shear strength of FS increased but was limited, and the shear strength of AABS showed a substantial increase. The overall strength showed a trend of first increasing and then decreasing with the increase in NaOH mass in AABS. The shear strength of AABS2 was the highest, and the shear strength of AABS was greater than that of FS.

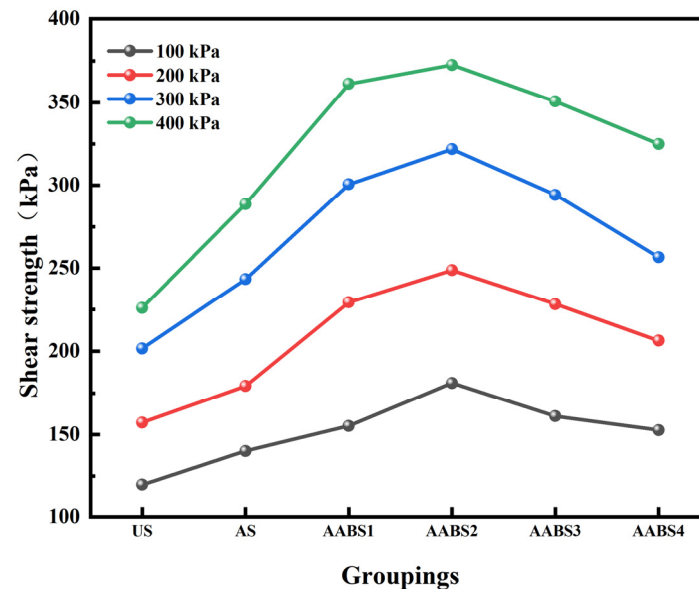


Figure 3. The shear strength of each group.

Figure 4 shows the variation in cohesion and friction angle of the soil samples. From the perspective of cohesion and internal friction angle, the values of expansive soil are the smallest, and there is a small increase in cohesion and the internal friction angle of FS. The internal friction angle and cohesion were further enhanced in AABS, with AABS1 reaching a maximum internal friction angle of 34.58° , followed by a decrease in internal friction

angle with the increase in NaOH. The cohesion of AABS2 was 109.09 kPa, which was the maximum among all groups, after which the cohesion also appeared to decrease with increasing NaOH. Friction angle and cohesion are important indicators of shear strength, and they jointly affect the magnitude of shear strength. The cohesion and internal friction angle of expansive soils are relatively minimal, so their shear strength is the lowest. AABS1 has a high friction angle but low cohesion, so the overall shear strength is not the highest. The analysis shows that the low content of NaOH makes the environment alkaline which cannot fully stimulate the low calcium fly ash to produce silicate gel, so the cohesion is not high enough. However, the generated gel can also promote the connection between soil and soil, and soil and fly ash [33], and the fly ash appears as microbeads, and the outer layer is destroyed in the alkaline environment, increasing the contact with the soil, thus increasing the internal friction angle. The NaOH in AABS2 can react with silica and alumina in fly ash to produce appropriate amounts of calcium silicate hydrate (C-S-H) gels and sodium aluminosilicate hydrate (N-A-S-H) gels. The gels can cement clay particles and fly ash, thus improving the cohesion and friction angle of AABS2. The excessive amount of NaOH in AABS4, means the surface layer of fly ash is destroyed, and the fly ash shows mutual fusion and gels small particles into large agglomerates, so the friction angle decreases. The excessive amount of NaOH destroys the adhesion between clay particles, so that the overall cohesion of AABS appears to decrease. The type of damage in AABS4 is similar to alkali contaminated clay [34].

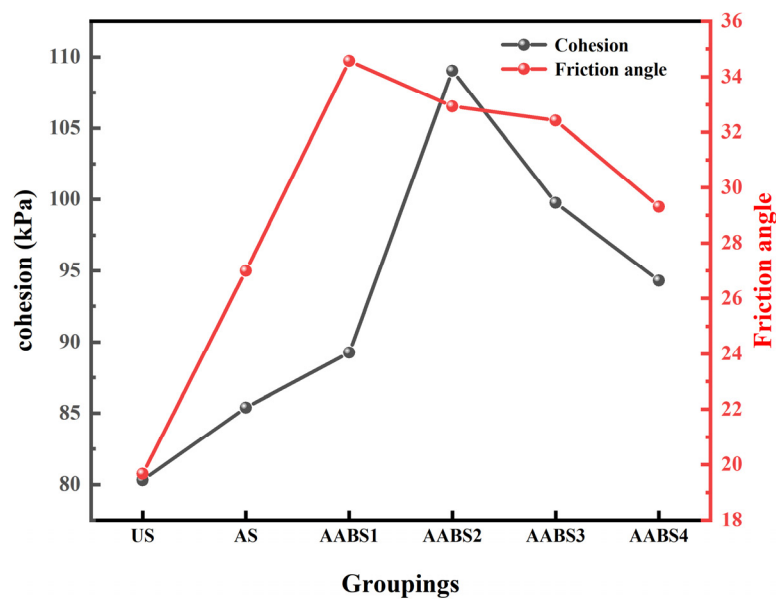


Figure 4. Cohesion and friction angle variation.

3.4. Unconfined Compressive Strength Test

Figure 5 represents the unconfined compressive strength of the groupings at different curing times and shows that the overall compressive strength seems to increase with the increase in curing time. When there is no curing, the FS strength increase is small and the increase is mainly from the fill of fly ash. The fine particle size of fly ash fills in the middle of the clay particles, improves the overall compactness of the soil sample and makes the compressive strength increase, but the increase is limited. In AABS, NaOH reacts with silica and alumina, respectively, and can generate C-S-H gels and N-A-S-H gels, but the products are not generated immediately, and need to react slowly over a period of time. Therefore, the strength of AABS does not increase significantly when it is not cured. When the content of NaOH is greater than 10% of the mass of fly ash, AABS will appear similar to alkali contaminated soil. The NaOH will corrode the clay particles and dissolve the cementing material in them, causing the internal structure of the soil to loosen and become brittle as a whole, resulting in a loss of strength [27,34].

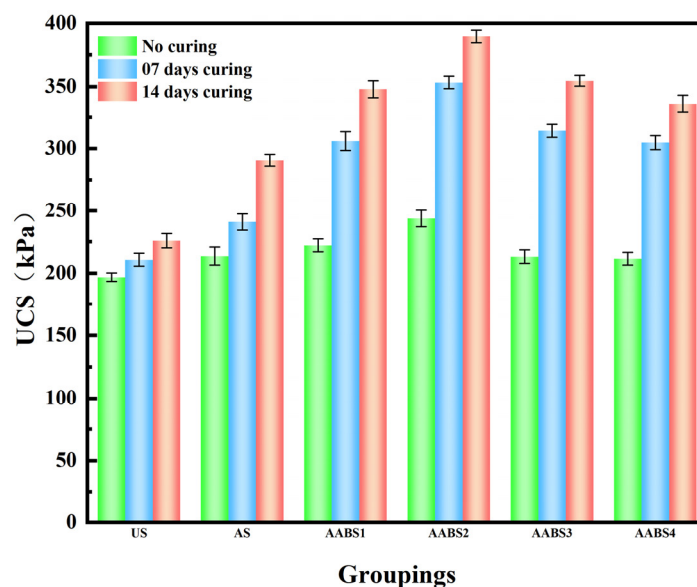


Figure 5. Unconfined compressive strength at 0 days, 7 days and 14 days of curing.

After 7 days of curing, the strength of all groups increased compared with those without curing. Poor early activity of FS leads to a slow reaction of volcanic ash, and strength increase comes from filling with fly ash on the one hand, and ion exchange on the other. The high valence ions Ca^{2+} , Mg^{2+} and Fe^{3+} in fly ash exchange with the low valence ions Na^+ and K^+ in the soil, reducing the thickness of the double electric layer around the soil particles, thus improving the flocculation around the clay particles [27]. The alkaline excitation of fly ash in AABS accelerates the alkali excitation reaction, and NaOH reacts with silica and alumina in fly ash to produce sodium silicate and sodium meta-aluminate, respectively, which are mixed to produce N–A–S–H gel. NaOH can also react with other metal ions in fly ash, which in turn accelerates the hydration reaction and hard coagulation. The generation of new substances such as N–A–S–H gel can enhance the internal association of the soil and form agglomerates, which causes the compressive capacity to increase significantly.

The compressive strength of FS was 213.6 kPa when not cured, and 290.7 kPa after 14 days of curing, which increased the strength by a total of 77.1 kPa or 36%. It can be seen in the figure that after 14 days of curing, the compressive strength of fly ash soil shows substantial increase, and it can be assumed that the rapid increase in strength of fly ash improved soil is after 7 days. This is because it takes some time to harden via its own solidification, and with the increase in curing time, the activity of fly ash is slowly excited in the soil, the alkali excitation reaction is intensified, and the generated silica–alumina gel fills the soil interior. This also proves that the early low-calcium fly ash is poorly active. The strength of AABS still grows, but slows down after 14 days of curing, and the strength of AABS is still higher than that of fly ash amended soil, which is because a large amount of hydrated calcium silicate, calcium silicate gel and hydrated calcium aluminate in the late stage of alkali excitation reaction binds with soil particles to form agglomerates, thus further improving the strength of the amended soil. At the end of the reaction, the hydrolysis products begin to solidify and harden, interlocking the soil's internal mosaic of compact structure, thus increasing the later strength.

According to two mechanical tests, it was found that there exists an optimum value for the amount of NaOH in AABS. Too little NaOH is not significant for strength enhancement, too much alkalinity also decreases the strength and the destruction results in brittleness. After comparing the swelling and mechanical properties, AABS2 was considered to have the best comprehensive effect. This conclusion is similar to the findings in [27,35,36].

3.5. Microstructure Analysis

To interpret the effect of AAB on the expansive soil further, US, FS and AABS2 were selected as representative soil samples for microscopic qualitative analysis by SEM. The following Figure 6 shows the images seen in US at different magnifications. Figure 6a shows that there are more pores and cracks on the surface of the expansive soil, and the internal denseness of the soil is very poor, and the pores are obviously irregularly arranged, and can easily become a water passage to make the soil swell. Figure 6 shows the images seen by US at different magnifications. The image in Figure 6a is magnified 500 times. There are more pores and penetrating cracks on the surface of the expansive soil, the internal denseness of the soil is extremely poor, and the pores are obviously irregularly arranged, which can easily become a channel for excess water to make the soil swell. The pores appear multi-layered on the surface of soil samples, and the soil samples of different layers are superimposed by face-to-face contact, and the overall view shows a wave pattern, which constitutes a turbulent structure, and is locally oriented and irregularly arranged as a whole. The image in Figure 6b is magnified 1000 times, and shows that the surface of the soil sample is curved, wrinkled and flattened, flattened less, mostly curved and wrinkled, and the interior of the soil is mostly blocky with smooth edges. The image in Figure 6c shows the surface of the soil sample at 2000 times magnification and the soil sample mostly exists in flakes with a curved shape, and an overall thick structure. Flocculating materials (centered on montmorillonite) can be found in the pores, and a small amount of montmorillonite is distributed on the flakes. In Figure 6d, the accumulation of lamellae on the surface of the soil sample can be observed at 3000 \times as stacked and scaled. The surface of the soil sample becomes aggregated into large particles, and the lamellae between the particles are stacked in face-to-face contact and the surface overlaps into edge-to-edge contact and edge-to-surface contact, and point-to-point contact mainly exists near the pores and cracks. Over all the expansive soil pores there are irregular structures and soil sample particles with large specific surface areas that easily combine with water, resulting in swellability.

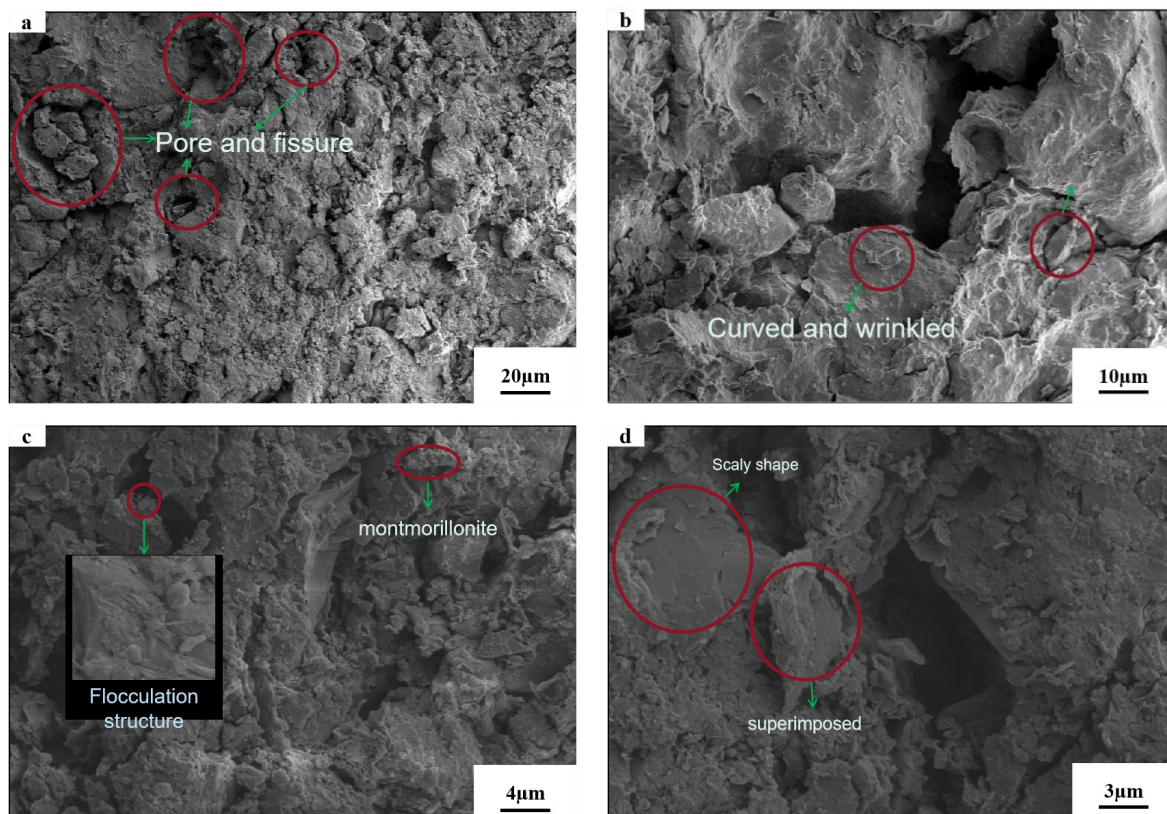


Figure 6. Typical scanning electron micrographs of US: (a) 500 \times ; (b) 1000 \times ; (c) 2000 \times ; (d) 3000 \times .

The microstructural morphology of FS is shown in Figure 7. The image in Figure 7a is magnified 500 times and the sample state of fly ash can be clearly observed, showing spherical microbead morphology. Because of the low viscosity of fly ash, the admixture of fly ash increases the proportion of non-viscous material that fills in the structural pores, making the FS relatively US denser. Fibrous gel can be observed on the surface of the soil sample, which is the result of the alkali excitation reaction of fly ash. Figure 7b shows the image with 1000 \times magnification, and it can be seen that under the adhesive effect of the gel, the fly ash and soil aggregate with each other and become larger aggregates. The large pores in the soil sample are filled and this promotes the compactness of the soil sample. Under the cementation of colloid, fly ash is embedded and fixed in the soil sample, and the flake structure and flocculent structure of the soil sample bond into a smooth and a smooth–massive structure. In Figure 7c, the fibrous gel image is magnified 2000 times, and it can be observed that the fibrous gel can overlap with each other and form a “bridge” between the fly ash and soil particles. It was also found that the generated gel can make the spherical fly ash stack on top of each other and become a whole. In Figure 7d, it can be observed that part of the gel clings to the fly ash and becomes the surface of the fly ash, thus increasing the viscosity and a higher adhesion to the soil particles. The addition of fly ash changed the original sample appearance of the soil sample, and the original flaky, stacked and fish scale surface of the soil sample disappeared and became a smoother surface.

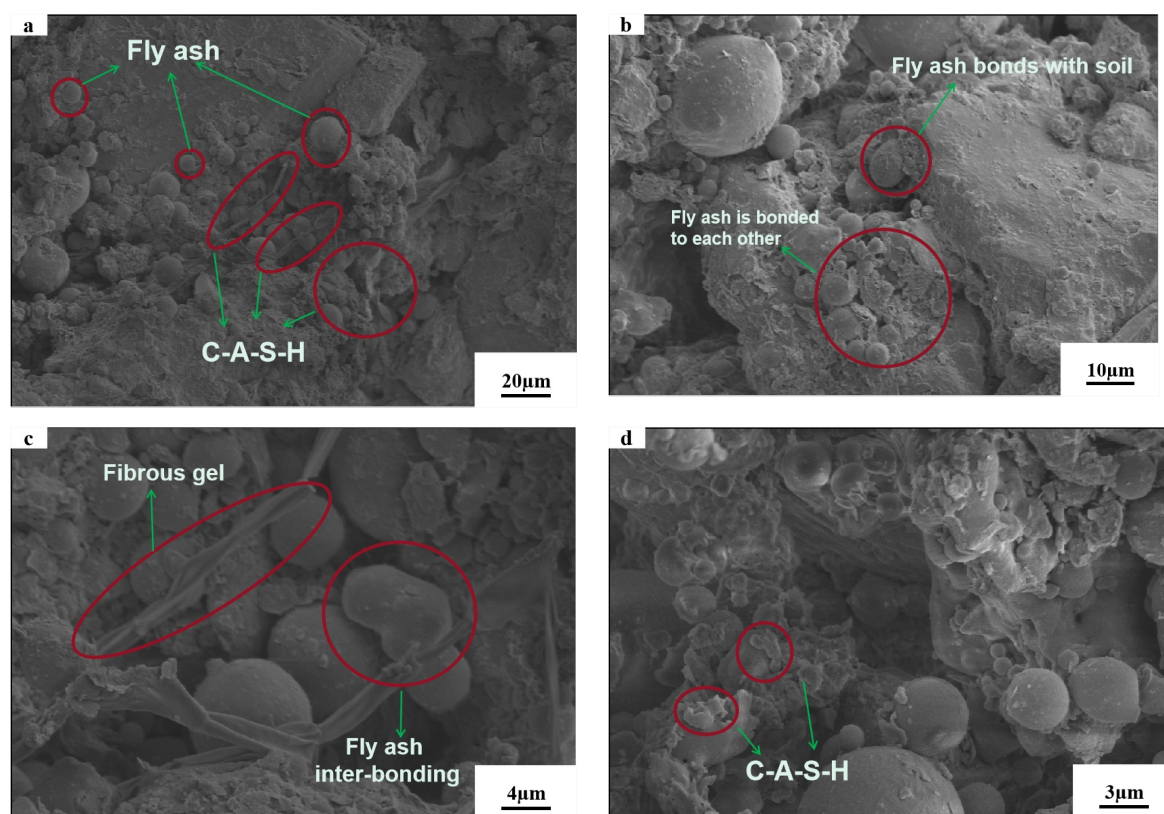


Figure 7. Typical scanning electron micrographs of FS: (a) 500 \times ; (b) 1000 \times ; (c) 2000 \times ; (d) 3000 \times .

In conclusion, for the FS after 14 days of curing, it can be found that the low-calcium fly ash has undergone an alkali excitation reaction in the soil, generating a small amount of gel attached to the fly ash surface or forming a fibrous filling in the pore space. The addition of fly ash on the one hand reduces the proportion of cohesive particles, which destroys the original structure of the expansive soil and makes the internal structural arrangement change. On the other hand, gel is located inside the soil to fill the pores and improve the overall compactness, so that the strength can be further improved, and the swelling can be

better resisted. However, fewer gels correspond to more limited strength increase. This is the same as result as the mechanical test conclusion.

Figure 8 shows the microscopic images of AABS2. In Figure 8a, the fly ash in the form of spherical microbeads is significantly reduced and the gel increases. The penetrating fractures are reduced, but new tiny pores are created in the gel adhesion. Figure 8b shows the image with 1000 times magnification, and it is possible to observe the fly ash that is participating in the reaction. At this time, the fly ash has an overall round shape, but the surface changes from smooth to rough, the NaOH erodes the surface and accelerates the release of activity, and there are gels and newly generated substances attached to the surface. Figure 8c shows the image magnified 2000 times, and a large fracture and many fine pores can be observed. It is thought that the newly generated objects such as calcium carbonate adsorbed by the gel have a filling effect on the small pores, and the effect on the large fractures is not obvious. It can also be seen that the surface layer of the soil sample is blocky as a whole, but the surface still shows smoothness in the area with few relevant reactions, and in the area with concentrated reactions, the surface is disordered and irregular. Figure 8d shows the image magnified 3000 times. It can be seen that calcium carbonate and colloid are adsorbed on the surface of the soil sample, making the smooth surface become irregular and cluttered.

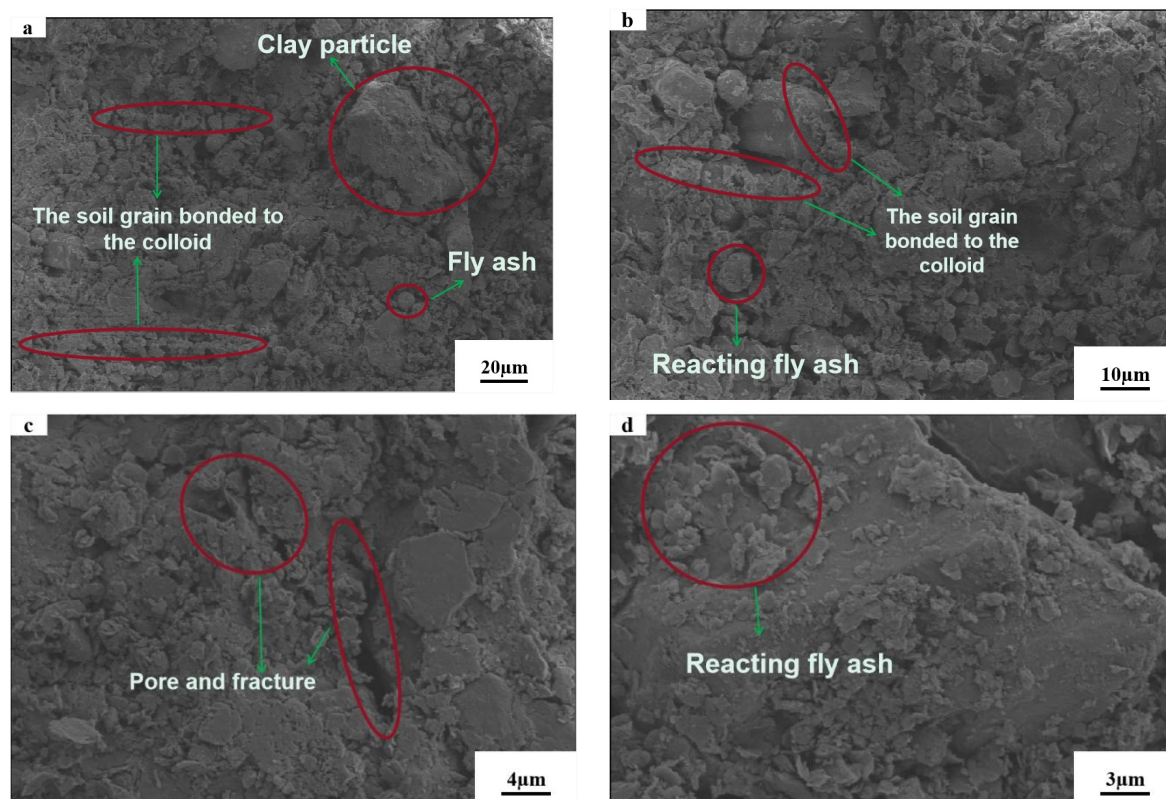


Figure 8. Typical scanning electron micrographs of AABS: (a) 500×; (b) 1000×; (c) 2000×; (d) 3000×.

Looking at the internal changes of AABS2 as a whole, it was found that the outer surface layer of fly ash is rapidly destroyed and the activity is released, accelerating the generation of substances such as gel and calcium carbonate, and the generated substances change the original structure of the soil sample and constitute a new irregularly ordered structure. AABS2 becomes more irregular, disorganized and finely fragmented internally in contrast to US. The stack and fish scale formed by sheet folding decreases, and the block formed by gel and clay-like agglomerate accumulation increases. The microstructure changes are similar to [37]. Long pores are reduced and more tiny pores and cracks are created in the agglomerate. Considering that too many tiny cracks and pores make the soil

sample brittle, the excessive addition of NaOH causes the soil to show overall brittleness and strength loss.

3.6. X-ray Diffraction XRD

Figure 9 shows the XRD test results of representative soil samples, i.e., the mineral composition of the samples. The presence of quartzite, calcite, montmorillonite and illite, tobermorite and beidellite can be observed in the soil. Quartz is chemically composed of silica, which comes from expanded clay and fly ash, and calcite is mainly composed of calcium carbonate, which comes from the reaction of calcium oxide in fly ash to produce an expansive clay. The presence of tobermorite $[\text{Ca}_5\text{Si}_6\text{O}_{16}(\text{OH})_2 \cdot 4\text{H}_2\text{O}]$ reveals the formation of reaction products, since the low crystalline C–S–H resembles the structure of this mineral [38]. Beidellite $(\text{Na}, \text{Ca})\text{Al}_2\text{Si}_4\text{O}_{10}(\text{OH})_2$ is formed by the presence of Ca^{2+} and Na^+ cations in the reaction during alkali activation [39]. The presence of heterodyne peaks between diffraction angles $20^\circ - 30^\circ$ (2θ) is attributed to disordered structures and highly amorphous contents (i.e., reaction products such as C–S–H and (C,N)–A–S–H [24,39]). The alkali excitation reaction can explain the formation of the above precipitates: (i) The dissolution of SiO_2 and Al_2O_3 in fly ash in a strong alkali environment; (ii) A small amount of CaO in fly ash reacts with silicate and aluminate monomers to form reaction products; (iii) Some CaO reacts with silicate and aluminate monomers to form C–A–S–H, and some CaO reacts with silicate monomers to form C–S–H; (iv) Na^+ is used to balance the charge and is absorbed by the silica–alumina phase to form N–A–S–H; (iv) Some Ca^{2+} may displace Na^+ to form C–A–S–H [19,40,41]. The presence of montmorillonite and illite is the reason for the swelling of expansive soils, which has been undetectable in FS and ABBS. It is thought that there are elements in the lattice of illite and montmorillonite that are replaced during chemical reactions, and Al^{3+} and Si^{4+} in Al–OH octahedra and Si–O tetrahedra in montmorillonite are easily replaced by low-valent ions such as Na^+ and Ca^{2+} in fly ash. SEM images (Figure 8) show the general morphology of the soil stabilized with the alkali-activated binder. In all SEM images, the soil is embedded in a cementitious matrix composed of reaction products. These products present a great compositional heterogeneity and amorphous structure, as seen in the XRD analysis. Results from the EDS analysis resulted in the chemical map (Figures 10b and 11b). They show, respectively, the proportion and concentration of the main chemical elements in the sample: silicon (Si), aluminum (Al), sodium (Na) and calcium (Ca). These elements are distributed in the mixtures and indicate the coexistence of C–S–H and (C,N)–A–S–H, the latter incorporating sodium cations from the activator [33].

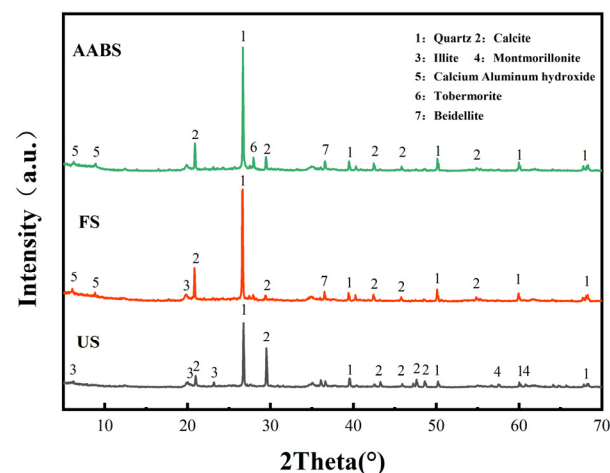


Figure 9. XRD patterns of US, FS and AABS2.

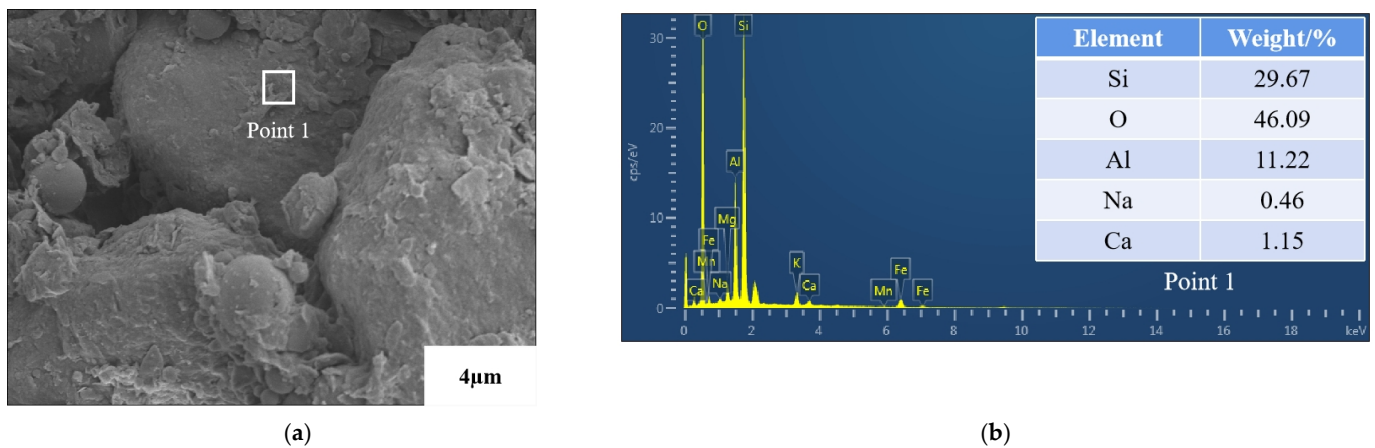


Figure 10. FESEM/EDS analysis of FS: (a) 3000 \times ; (b) chemical map.

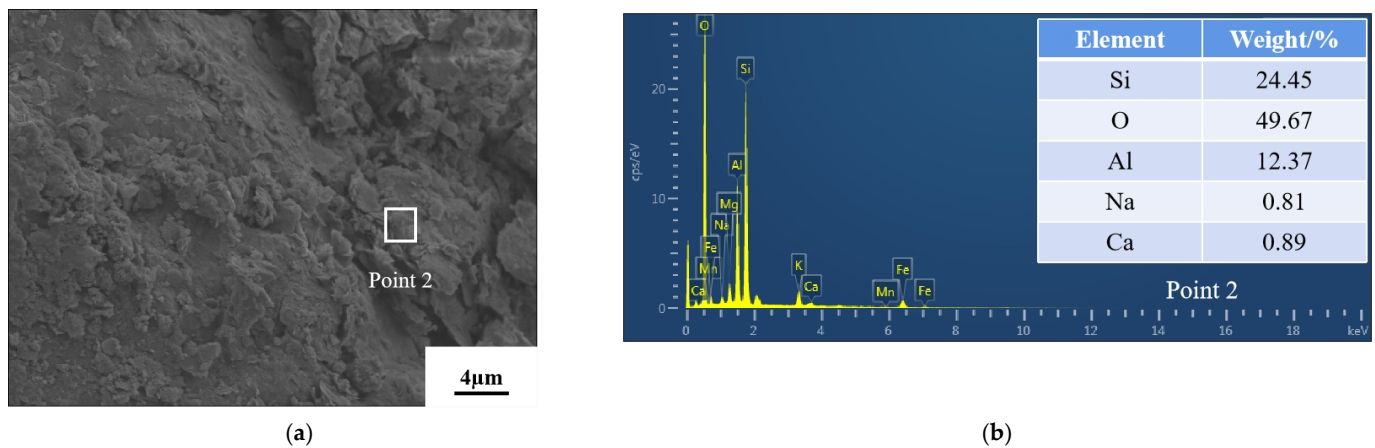


Figure 11. FESEM/EDS analysis of ABBS2: (a) 3000 \times ; (b) chemical map.

4. Conclusions

This study examines the stabilization of expansive soil by NaOH excited fly ash as a binder, which can consume solid waste, protect the environment, and provide a new solution to replace cement and other substances. In this study, different amounts of NaOH excited fly ash were selected to stabilize the expansive soils and to find the optimal NaOH content to reduce the expansiveness of the soils and to improve the strength of the soils. The following conclusions were obtained:

1. According to the unloaded swelling test and the loaded swelling test, it was found that AAB can further reduce the swelling property of the soil, but the swelling property does not change significantly when the NaOH content is greater than 8%.
2. According to the straight shear test and unconfined compressive strength test, AAB can improve the mechanical strength of soil, AABS2 can reach the maximum strength, and more NaOH will make the soil sample brittle and cause strength to decline. Excess NaOH decreases the cohesion and friction angle.
3. Microscopic tests demonstrated that the reactions in AAB produced C–S–H and (C,N)–A–S–H, and that the new substances generated changed the internal structural arrangement of the soil, filled the pores and created adhesion with the clay. After the gel was hydrated and hardened, the high strength of the soil was ensured and the newly generated gel wraps around the clay particles, thus suppressing the swelling properties.
4. This study proposed an eco-friendly sustainable binder, which can be used to improve the performance of expansive soil.

Author Contributions: Methodology, H.W. and C.Y.; validation, T.L. and C.Y.; formal analysis, T.L.; investigation, H.W.; data curation, T.L.; writing and original draft preparation, T.L.; writing—review and editing, H.W. and J.W. All authors have read and agreed to the published version of the manuscript.

Funding: This research received no external funding.

Institutional Review Board Statement: Not applicable.

Informed Consent Statement: Not applicable.

Data Availability Statement: The data presented in this study are available on request, from the corresponding author.

Conflicts of Interest: We declare that we do not have any commercial or associative interest that represents a conflict of interest in connection with work submitted.

References

- Chen, F.H. *Foundations on Expansive Soils*; Elsevier: Amsterdam, The Netherlands, 1975.
- Mazhar, S.; Anasua, G.; Divyam, G. Strength characterisation of fiber reinforced expansive subgrade soil stabilized with alkali activated binder. *Road Mater. Pavement*. **2021**, *23*, 1037–1060. [[CrossRef](#)]
- Yi, Y.; Gu, L.; Liu, S. Microstructural and mechanical properties of marine soft clay stabilized by lime-activated ground granulated blast furnace slag. *Appl. Clay Sci.* **2015**, *103*, 71–76. [[CrossRef](#)]
- Puppala, A.J.; Pedarla, A. Innovative ground improvement techniques for expansive soils. *Innov. Infrastruct. Solut.* **2017**, *2*, 24. [[CrossRef](#)]
- Woldesenbet, T.T. Experimental Study on Stabilized Expansive Soil by Blending Parts of the Soil Kilned and Powdered Glass Wastes. *Adv. Civ. Eng.* **2022**, *12*, 96455589. [[CrossRef](#)]
- Zha, F.; Liu, S.; Du, Y.; Cui, K. Behavior of expansive soils stabilized with fly ash. *Nat. Hazards* **2008**, *47*, 509–523. [[CrossRef](#)]
- Jones, L.D.; Jefferson, J. *ICE Manual of Geotechnical Engineering Volume 1: Geotechnical Engineering Principles, Problematic Soils and Site Investigation*; The National Academies of Sciences, Engineering, and Medicine: Washington, DC, USA, 2012.
- Kamei, T.; Ahmed, A.; Ugai, K. Durability of soft clay soil stabilized with recycled Bassanite and furnace cement mixtures. *Soils Found.* **2013**, *53*, 155–163. [[CrossRef](#)]
- Higgins, D. Briefing: GGBS and sustainability. *Const. Mater.* **2007**, *160*, 99–101. [[CrossRef](#)]
- Shihab, A.M.; Abbas, J.M.; Ibrahim, A.M. Effects of temperature in different initial duration time for soft clay stabilized by fly ash based geopolymer. *Civ. Eng. J.* **2018**, *4*, 2082–2096. [[CrossRef](#)]
- Suhendro, B. Toward green concrete for better sustainable environment. *Procedia Eng.* **2014**, *95*, 305–320. [[CrossRef](#)]
- Krivenko, P. Why alkaline activation—60 years of the theory and practice of alkali-activated materials. *J. Ceram. Sci. Technol.* **2017**, *8*, 323–333. [[CrossRef](#)]
- Davidovits, J. False values on CO₂ emission for geopolymer cement/concrete published in Scientific Papers. *Geopolym. Inst. Libr. Tech. Pap.* **2015**, *24*, 1–9.
- Palomo, A.; Krivenko, P.; Garcia-Lodeiro, I.; Kavalerova, E.; Maltseva, O.; Fernández-Jiménez, A. A review on alkaline activation: New analytical perspectives. *Mater. Construcc.* **2014**, *64*, 315. [[CrossRef](#)]
- Jia, Z.; Yang, Y.; Yang, L.; Zhang, Y.; Sun, Z. Hydration products, internal relative humidity and drying shrinkage of alkali activated slag mortar with expansion agents. *Constr. Build. Mater.* **2018**, *158*, 198–207. [[CrossRef](#)]
- Yi, Y.; Li, C.; Liu, S. Alkali-activated ground-granulated blast furnace slag for stabilization of marine soft clay. *J. Mater. Civ. Eng.* **2015**, *27*, 4. [[CrossRef](#)]
- Rivera, J.F.; Orobio, A.; Mejía, R.; Cristelo, N. Clayey soil stabilization using alkali-activated cementitious materials. *Mater. Constr.* **2020**, *70*, 211. [[CrossRef](#)]
- Miraki, H.; Shariatmadari, N.; Ghadir, P.; Jahandari, S.; Tao, Z.; Siddique, R. Clayey soil stabilization using alkali-activated volcanic ash and slag. *J. Rock Mech. Geotech. Eng.* **2022**, *14*, 576–591. [[CrossRef](#)]
- Syed, M.; GuhaRay, A.; Kar, A. Stabilization of expansive clayey soil with alkali activated binders. *Geotech. Geol. Eng.* **2020**, *38*, 6657–6677. [[CrossRef](#)]
- Adeyanju, E.; Okeke, C.A.; Akinwumi, I.; Busari, A. Subgrade stabilization using rice husk ash-based geopolymer (GRHA) and cement kiln dust (CKD). *Case Stud. Constr. Mater.* **2020**, *13*, 00388. [[CrossRef](#)]
- Bruschi, G.J.; dos Santos, C.P.; de Araújo, M.T.; Ferrazzo, S.T.; Marques, S.; Consoli, N.C. Green stabilization of bauxite tailings: A mechanical study on alkaliactivated materials. *J. Mater. Civ. Eng.* **2021**, *31*, 11. [[CrossRef](#)]
- Bruschi, J.; dos Santos, C.P.; Ferrazzo, S.T.; de Araújo, M.T.; Consoli, N.C. Parameters controlling loss of mass and stiffness degradation of green stabilized bauxite tailings. *Proc. Inst. Civ. Eng.-Geotech. Eng.* **2021**, *62*, 177–183. [[CrossRef](#)]
- Pannirselvam, N.; Chandramouli, K.; Anitha, V. Pulse Velocity Test on BananaFibre Concrete with Nano Silica. *Int. J. Civ. Eng. Technol.* **2018**, *9*, 2853–2858.

24. Kar, A.; Halabe, U.B.; Ray, I.; Unnikrishnan, A. Nondestructive characterizations of alkali activated fly ash and/or slag concrete. *Eur. Sci. J. ESJ* **2013**, *9*, 52–74. [[CrossRef](#)]
25. Horpibulsuk, S.; Phetchuay, C.; Chinkulkijniwat, A. Soil stabilization by calcium carbide residue and fly ash. *J. Mater. Civ. Eng.* **2012**, *24*, 184–193. [[CrossRef](#)]
26. Miao, S.; Shi, J.; Sun, Y.; Zhang, P.; Shen, Z.; Nian, H. Mineral abundances quantification to reveal the swelling property of the black cotton soil in Kenya. *Appl. Clay Sci.* **2018**, *161*, 524–532. [[CrossRef](#)]
27. Gupta, S.; GuhaRay, A.; Kar, A.; Komaravolu, V.P. Performance of alkali-activated binder-treated jute geotextile as reinforcement for subgrade stabilization. *Int. J. Geotech. Eng.* **2018**, *15*, 298–312. [[CrossRef](#)]
28. Bunaciu, A.A.; Udriștioiu, E.G.; Aboul-Enein, H.Y. X-ray Diffraction: Instrumentation and Applications. *Crit. Rev. Anal. Chem.* **2015**, *45*, 289–299. [[CrossRef](#)]
29. Das, R.; Eaqub, A.; Hamid, A.; Bee, S. Current applications of x-ray powder diffraction—A review. *Rev. Adv. Mater. Sci.* **2014**, *38*, 95–109.
30. Mohammed, A.; Abdullah, A. Scanning Electron Microscopy (SEM): A Review. In Proceedings of the 2018 International Conference on Hydraulics and Pneumatics, Băile Govora, Romania, 7–9 November 2018.
31. Mypati, V.; Sireesh, S. Feasibility of Alkali-Activated Low-Calcium Fly Ash as a Binder for Deep Soil Mixing. *J. Mater. Civil. Eng.* **2021**, *34*, 04021410. [[CrossRef](#)]
32. Alsafi, S.; Farzadnia, N.; Asadi, A.; Huat, B.K. Collapsibility potential of gypseous soil stabilized with fly ash geopolymer; characterization and assessment. *Constr. Build. Mater.* **2017**, *137*, 390–409. [[CrossRef](#)]
33. Darius, Z.; Danute, V.; Stelmokaitis, G.; Viktoras, D. Clayey Soil Strength Improvement by Using Alkali Activated Slag Reinforcing. *Minerals* **2020**, *10*, 1076. [[CrossRef](#)]
34. Yu, S.; Xuejue, C.; Jie, A. Experimental study on the deformation characteristics and microstructure of clay polluted by alkaline solution. *China Sci. Pap.* **2015**, *10*, 1578–1582.
35. Parhi, P.S.; Garanayak, L.; Mahamaya, M. Stabilization of an Expansive Soil Using Alkali Activated Fly Ash Based Geopolymer. In *Sustainable Civil Infrastructures*; Springer: Cham, Switzerland, 2018; pp. 36–50. [[CrossRef](#)]
36. Santhikala, R.; Chandramouli, K.; Pannirselvam, N. Stabilization of expansive soil using fly ash based geopolymer. *Mater. Proc.* **2022**, *68*, 110–114. [[CrossRef](#)]
37. Alemshet, D.; Fayissa, B.; Geremew, A. Amelioration Effect of Fly Ash and Powdered Ground Steel Slag for Improving Expansive Subgrade Soil. *Oxid. Med. Cell. Longev.* **2023**, *10*, 1700857. [[CrossRef](#)]
38. Zailani, W.W.A.; Bouaissi, A.; Fansuri, H. Bonding Strength characteristics of FA-based geopolymer paste as a repair material when applied on OPC substrate. *Appl. Sci.* **2020**, *10*, 3321. [[CrossRef](#)]
39. Kar, A.; Ray, I.; Halabe, U.B.; Unnikrishnan, A.; Dawson-Andoh, B. Characterizations and quantitative estimation of alkali-activated binder paste from microstructures. *Int. J. Concr. Struct. Mater.* **2014**, *8*, 213–228. [[CrossRef](#)]
40. García-Lodeiro, I.; Fernández-Jiménez, A.; Palomo, A. Hydration kinetics in hybrid binders: Early reaction stages. *Cem. Concr. Compos.* **2013**, *39*, 82–92. [[CrossRef](#)]
41. Ma, H.; Zhu, H.; Yi, C.; Fan, J.; Chen, H.; Xu, X.; Wang, T. Preparation and reaction mechanism characterization of alkali-activated coal gangue-slag materials. *Materials* **2019**, *12*, 2250. [[CrossRef](#)]

Disclaimer/Publisher’s Note: The statements, opinions and data contained in all publications are solely those of the individual author(s) and contributor(s) and not of MDPI and/or the editor(s). MDPI and/or the editor(s) disclaim responsibility for any injury to people or property resulting from any ideas, methods, instructions or products referred to in the content.